Bulk thermal polymerisation of diethylene glycol bis(allyl carbonate) as studied by dielectric relaxation spectroscopy

Ian K. Smith,[a] Stuart R. Andrews,[a] Graham Williams*[a] and Paul A. Holmes[b]

[a]*Department of Chemistry, University College of Swansea, Singleton Park, Swansea, UK SA2 8PP*

[b]*Pilkington Technology Management Limited, Hall Lane, Lathom, Ormskirk, Lancashire, UK L40 5UF*

Broad-band dielectric relaxation spectroscopy (DRS) has been used to study the changes in molecular relaxation behaviour when diethylene glycol bis(allyl carbonate) (CR39 monomer) is polymerised thermally in its bulk state. As polymerisation proceeds the dielectric α-relaxation process broadens markedly and moves to higher temperatures while, at the same time, a small low-temperature β-relaxation process increases in its intensity and moves to higher temperatures. The dielectric loss spectra are shown to provide a convenient fingerprint that indicates the extent of cure in partially cured materials.

Polymer glasses formed from the CR39 monomer are used widely as materials for prescription lenses, safety glasses and as synthetic glasses in a variety of applications because of their excellent optical clarity and mechanical strength. Few studies have been reported on the nature of the free-radical polymerisation of the CR39 monomer. Dial *et al.*[1] used idiometry as a method to analyse the polymerisation kinetics, while Schnarr and Russell[2] used dilatometry to study the early stages of polymerisation. Starkweather and Eirich[3] also used dilatometry while Hill *et al.*[4] used density and refractive index methods together with NIR and EPR spectroscopies to monitor the polymerisation process. While such methods provide essential information on changes in physical and chemical structures during polymerisation, they are fairly insensitive to the important changes in the mechanical properties that occur in the late-stages of cure that lead to glass formation. The technique of dielectric relaxation spectroscopy (DRS) provides a convenient and sensitive means of monitoring changes in that range, since it provides information on molecular motions of chain dipoles in the developing cross-linked network. De Meuse[5,6] reported dielectric studies of the polymerisation of the CR39 monomer. Two relaxation processes were observed in the cured polymer glass: (i) an α-relaxation process associated with the glass transition, and (ii) a β-relaxation process due to localised motions of ether and carbonyl dipoles. He showed[6] that the location of the dielectric β-process in plots of loss factor (ε'') *vs.* temperature (T) was sensitive to the cure cycle used and the initiator employed. Frounchi *et al.*,[7] using dynamic-mechanical relaxation methods, studied the cured polymer and observed α- and β-processes in the region of 100 °C and −50 °C, respectively.

In the present work, we present extensive dielectric data for materials polymerised to different extents, starting with the uncured CR39 monomer, which is a glass forming liquid, extending to the fully cured polymer glass. The variations of the different dielectric relaxation processes with sample preparation are documented and are shown to provide a convenient means of monitoring the state of cure of samples. In an earlier paper[8] we reported the dielectric relaxation behaviour of CR39 monomer as studied over the frequency range 10^{-2} to 10^{4} Hz and the temperature range −110 °C to −50 °C, giving information on the α-relaxation process, its form and dependence on temperature.

Experimental

The CR39 monomer (see Fig. 1) was polymerised in its bulk state using diisopropyl peroxydicarbonate (IPP, see Fig. 1) as the free-radical initiator. The materials were supplied by Akzo Chemicals and used in their as-received state without further purification. A 3% solution of IPP in CR39 monomer was prepared and portions were used for all subsequent studies reported here. The dielectric measurements were made using a Novocontrol dielectric spectrometer that incorporated a Solartron SI 1260 impedance/gain-phase analyser with a Chelsea dielectric interface, allowing measurements of the complex permittivity, $\varepsilon^* = \varepsilon'(\omega) - i\varepsilon''(\omega)$ in the frequency range 10^{-3} to 10^{6} Hz. Fig. 2 shows a schematic diagram of the measuring system. The Novocontrol Quatro unit controlled sample temperature using N_2 gas and allowed measurements to be made in the range −180 to 400 °C with a precision of 0.1 °C. The measuring system was computer controlled using the Novocontrol WinDETA software, allowing a wide range of heating/cooling cycles and frequency sweeps to be made automatically. The liquid monomer was placed in a brass cup with an inside diameter of 36 mm, which formed the lower

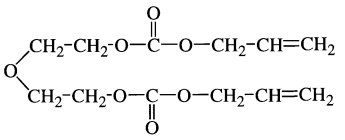

Fig. 1

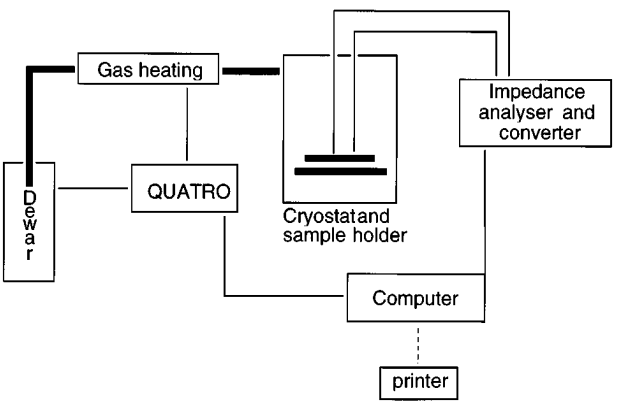

Fig. 2

Table 1 The CR39 cure cycle showing the stages up to which different samples of the master solution were cured

cure temperature/°C	cure time/h, min	product
40	16,00	P1
45	16,20	
50	16,40	
55	17,00	P2
60	17,20	
65	17,40	
70	18,00	P3
75	18,20	
80	18,40	P4
85	21,00	
90	21,20	
95	21,40	
100	22,00	
105	22,20	
110	22,40	
115	23,00	
120	44,00	P6

electrode, and a brass disc of 30 mm diameter was placed on top and acted as the upper electrode. The electrode separation was maintained by two thin strips of PTFE, thickness 760 μm. This electrode assembly was mounted in the Novocontrol BDS1200 sample holder which was placed in the cryostat head of the instrument. Calculations of the permittivity, ε', and loss factor, ε'', for the sample in the cell were made using standard sample-out and sample-in measurements of the cell equivalent parallel capacitance and conductance at each frequency. In a frequency sweep, measurements were made at 51 frequencies in the range 10 to 10^5 Hz, while in a temperature scan measurements were made at 3 °C intervals in the range −130 to 100 °C. Each measurement of (ε', ε'') at each frequency and temperature was recorded during each experiment thus allowing post processing of data to give [$\varepsilon''(f,T)$, $\varepsilon''(f,T)$] for each data point for use in two- and three-dimensional plots.

Samples were polymerised as follows. A portion of the master solution (3% IPP in CR39 monomer) was placed in the dielectric cell and then incorporated into the measuring system as described above. It was then heated according to the cure cycle given in Table 1, up to a chosen point and then cooled rapidly to −130 °C which stopped the reaction (*e.g.* sample P2 was obtained by heating a portion of the sample mixture for 16 h at 40 °C, followed by 20 min at 45 °C, 20 min at 50 °C and finally 20 min at 55 °C, then rapid cooling that sample to −130 °C). It was then studied as a function of frequency during a heating run at every 3 °C in the range 130 °C to T_{end}, where T_{end} is chosen to be sufficiently high for a sample to allow full characterisation of the dipole relaxation processes.

Reaction mechanism and dielectric behaviour

It is appropriate to describe the essential chemical processes involved in the thermal free-radical polymerisation of the CR39 monomer. The initiator material IPP is effective in the range 35–50 °C. On heating the reaction mixture to temperatures in this range, IPP decomposes into two free radicals which then initiate the polymerisation in the usual way, by adding to the C=C bond of the allyl group of the CR39 monomer. Since the CR39 monomer is bifunctional, the resulting propagating chain will have side-groups that contain active C=C groups. During polymerisation, an intramolecular cyclisation reaction may occur[2,9] (Scheme 1). During the initial stages of the reaction this has been shown[1] to occur only to a slight extent in comparison with the main addition process. In addition, Holt and Simpson[9] have shown that the extent of intramolecular cyclisation is inversely dependent on the initial monomer concentration and the distance between the two allyl groups.

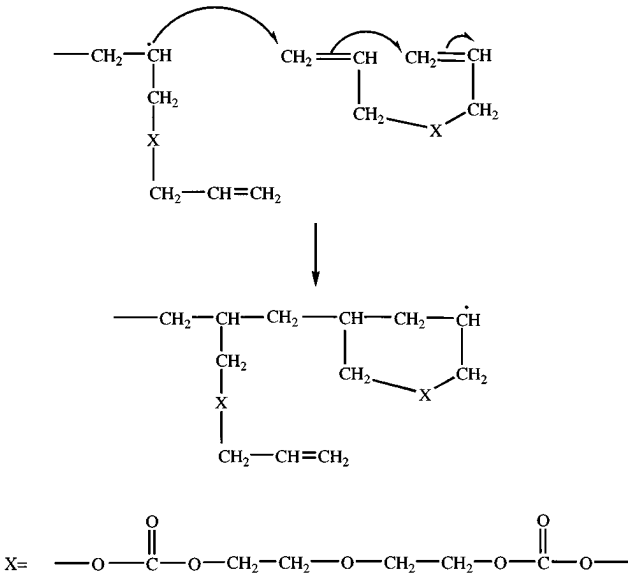

Scheme 1 Intramolecular cyclisation

Since for our system we have a concentrated monomer solution (97%) and the distance between the two allyl groups in the monomer is relatively large,[9] then the cyclisation reaction only occurs to a small extent.

A general feature in the polymerisation of allyl monomers is a chain transfer reaction (Scheme 2) in which the growing chain ($P_n^{\cdot}$) is terminated and an allyl radical is produced. Since such species are resonance stabilised, they are less likely to cause further chain growth than chain termination by combination with other propagating radicals or similar allyl radicals. When this occurs the chain transfer reaction it is termed degrative since it leads to termination of the growing chains. For this reason degrative chain transfer is perhaps the most important kinetic step in the polymerisation of the CR39 monomer. Hill *et al.*[4] have shown that the major radical species present at conversions below 45% is the allyl radical. However, Starkweather and Eirich[3] have shown that during the later stages of the reaction, the importance of the degrative chain transfer is less prevalent in the polymerisation of diallyl compounds than monoallyl compounds, and have shown that the ultimate conversion of double bonds for the CR39 monomer is greater than that expected. This is explained as being due to reinitiation caused by the allyl radicals. At the later stages of cure, a three-dimensional network of cross-linked polymer chains is formed in which reactions involving a propagating radical and a vinyl group will become progressively more difficult. Active species will become isolated from each other since they are chemically bonded to the network. Such a network will contain unreacted vinyl groups together with allyl radicals. Thus, the allyl radicals are less likely to cause chain termination by combination with other radical species than a reaction with the unreacted C=C bonds causing reinitiation (Scheme 3). The importance of reinitiation has also been recognised by other workers in other studies of diallyl polymerisation.[10–12] Thus in the later stages of the reaction

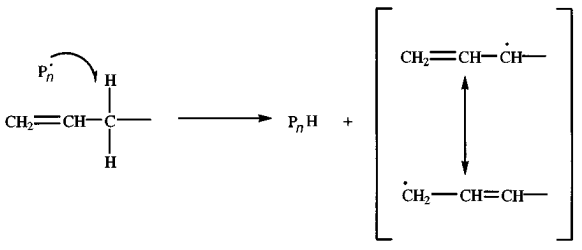

Scheme 2 Chain transfer

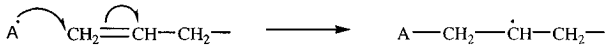

Scheme 3 Reinitiation of the reaction by the allyl A˙ radical

the allyl radicals are an important source of cross-linking reactions and the decrease in the concentration of C=C bonds in the system.

In a previous publication[8] by our group, it was shown that the glass-forming CR39 monomer liquid exhibited a well defined α-relaxation due to the large-scale reorientational motions of the dipoles, and a weakly defined β-relaxation due to the localised motions of the dipoles. Therefore, in relation to the dielectric properties of the reacting system, we expect to observe multiple relaxation processes associated with the large-scale and localised motions of the ester and ether dipoles, which of course throughout the reaction remain chemically unchanged.

The complex permittivity of a material can be expressed using a Fourier transform relation[13] according to eqn. (1):

$$\frac{\varepsilon^*(\omega)-\varepsilon_\infty}{\varepsilon_0-\varepsilon_\infty}=1-i\omega\int_0^\infty \phi(t)\exp(-i\omega t)\mathrm{d}t \qquad (1)$$

where $\omega=2\pi f/\mathrm{Hz}$, ε_0 and ε_∞ are the limiting low and high frequency permittivities with respect to the relaxation range, and $\phi(t)$ is a decay function for the polarisation that describes the relaxation of a material following the step-removal of an electric field. To a good approximation $\phi(t)$ corresponds to the dipole moment correlation function $C_\mu(t)$, for the reorientational motions of dipoles in a material[14,15] which may be written as:

$$C_\mu(t)=\frac{\sum_{i,j}^{N}<\mu_i(0)\mu_j(t)>}{\sum_{i,j}^{N}<\mu_i(0)\mu_j(0)>} \qquad (2)$$

Here the sum is taken over all dipoles N in a macroscopic volume V in the material. In regards to the system studied here, eqn. (2) contains autocorrelation terms for the motions of ether and ester dipoles (μ_{ether}, μ_{ester}) and cross-correlation terms between the two dipoles. As explained in detail for glass-forming liquids and polymers,[16] the motions of such dipoles may occur by local processes that only partially randomise the dipole vector, giving rise to secondary (β, γ, *etc.*) dielectric relaxations, or by micro-Brownian motions (α-process) that totally relax the remainder of the mean square dipole moment not relaxed by the secondary processes. Thus, a dielectric study of the uncured, partially cured and fully cured CR39 monomer materials will provide valuable information on how the motions of the dipoles are affected by the extent of polymerisation and cross-linking.

Results and Discussion

We have already shown that the CR39 monomer exhibits a well defined α-relaxation process. The frequency of maximum dielectric loss factor in plots of ε'' *vs.* $\log(f/\mathrm{Hz})$ obeys the Vogel–Fulcher equation,

$$\log(f)=f_0-\left[\frac{B}{T-T_0}\right] \qquad (3)$$

with parameters $f_0=13.09$, $B=1236$ K and $T_0=147.4$ K. On polymerisation the reaction mixture contains a range of polymeric species in addition to the unreacted monomer. Fig. 3(*a*) and (*b*) shows three-dimensional plots of ε' and ε'' as a function of frequency and temperature for the least cured product P1 (Table 1). One dipole relaxation process is clearly observed together with a rising loss process at low frequencies and high temperatures due to ionic conduction in the material.

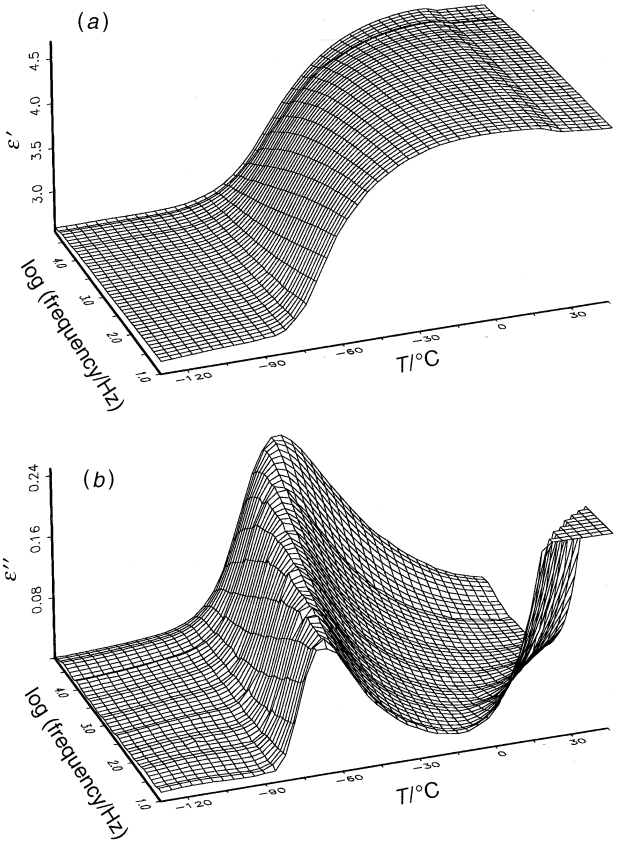

Fig. 3 (*a*) Permittivity and (*b*) loss as a function of frequency and temperature for P1

Comparison of these data with those reported for the monomer[8] shows that the α-loss peak has moved to higher temperatures by *ca.* 20 °C, reflecting an increased T_g for this partially cured material, and has broadened significantly in both the frequency and temperature domains, reflecting that dipole motions are now occurring in a range of local environments in this material (see also the discussion of Fig. 6 below). Fig. 4(*a*) and (*b*) shows data for sample P4. Comparison of the permittivity data shows that although the high-temperature permittivities are approximately the same for both samples (and for the CR39 monomer[8]) the breadth of the dielectric dispersion is increased markedly by further curing. The complementary loss data in Fig. 4(*b*) shows how broad the α-process has become and how the shift of the process to higher temperatures is continued. Importantly, a small loss feature is observed at low temperatures and frequencies, which at 10 Hz is centred at *ca.* −100 °C. Fig. 5(*a*) and (*b*) shows data for sample P6. The permittivity curves show a gradual decrease from the high-temperature values for $T\approx100$ °C and a small but definite low-temperature dispersion region is now apparent below −80 °C. The loss data in Fig. 5(*b*) show a complex pattern of behaviour and it is apparent that the low-temperature process is enhanced further and the high-temperature process is extremely broad and has continued to move to higher temperatures than in sample P4. The qualitative features of Fig. 3–5, taken together with our earlier results[8] for the CR39 monomer (Fig. 3 of ref. 8) may be summarised as follows.

(1) The magnitude of the dielectric dispersion for the mixtures of dipoles, $\Delta\varepsilon=\varepsilon(\mathrm{high}\ T)-\varepsilon(\mathrm{low}\ T)$, does not change markedly as the monomer is polymerised. Thus, although the nature and timescale for the motions of ether and ester dipoles changes markedly, the spatial extent of their overall motions is not changed appreciably when a comparison is made at a fixed high temperature (*e.g.* 120 °C) say, which is above the T_g of all samples.

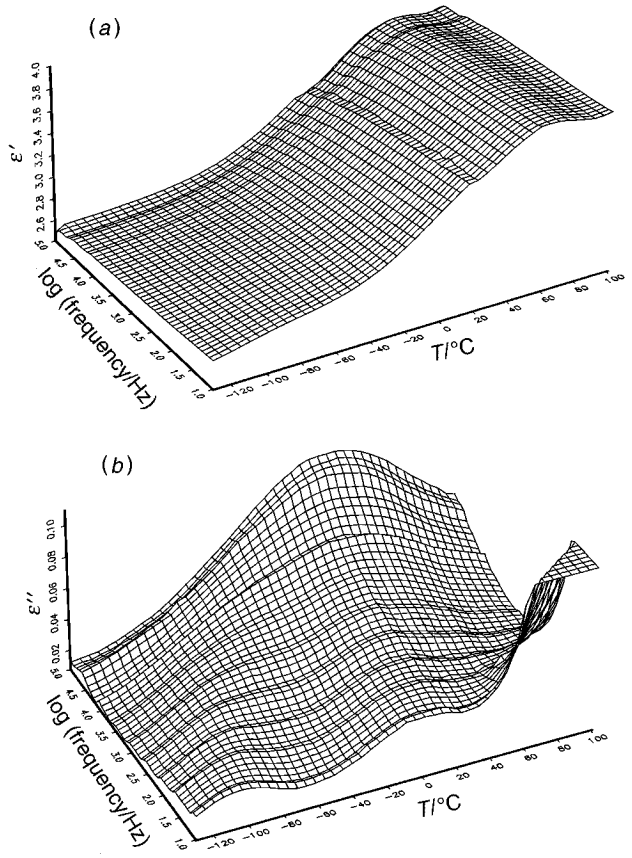

Fig. 4 (*a*) Permittivity and (*b*) loss as a function of frequency and temperature for P4

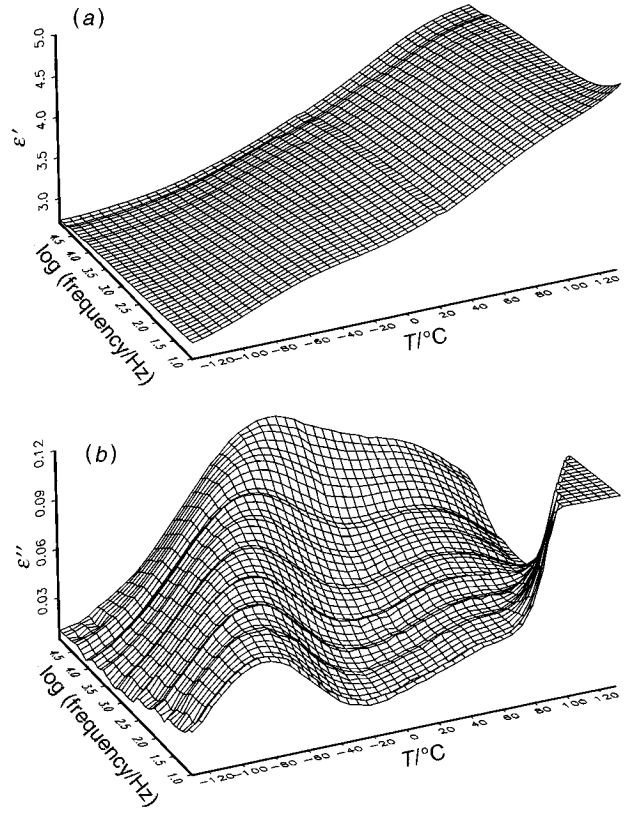

Fig. 5 (*a*) Permittivity and (*b*) loss as a function of frequency and temperature for P6

(2) The three-dimensional dielectric landscapes provided by the figures reveal changes taking place in relaxation processes that were not readily obtainable previously (although Reddish in early studies of the dielectric behaviour of polyethylene terephthalate had previously given a three-dimensional representation of the loss data as a function of frequency and temperature, see ref. 3). From the loss data in Fig. 3–5 we see (i) that the α-process broadens remarkably and its location moves to higher temperatures and (ii) a new low-temperature β-process appears and increases in relaxation strength with increased curing. While the loss peaks for the α- and β-processes are clearly defined in the temperature domain in all cases, the loss peaks become so broad in the frequency domain for samples P3–P6 that it is difficult to determine the frequency of maximum loss in such cases.

We consider first the changes in plots of ε'' *vs.* T at fixed frequencies for the different samples. Fig. 6(*a*) shows the data for CR39 monomer together with those for P1, P2 and P3 all measured at 1 kHz. The height of the α-loss peak decreases from 0.61 to 0.165 to 0.125 on going from the monomer through to P3. Fig. 6(*b*) shows the results for P1–P3 on an expanded scale that reveals the emergence of the β-process

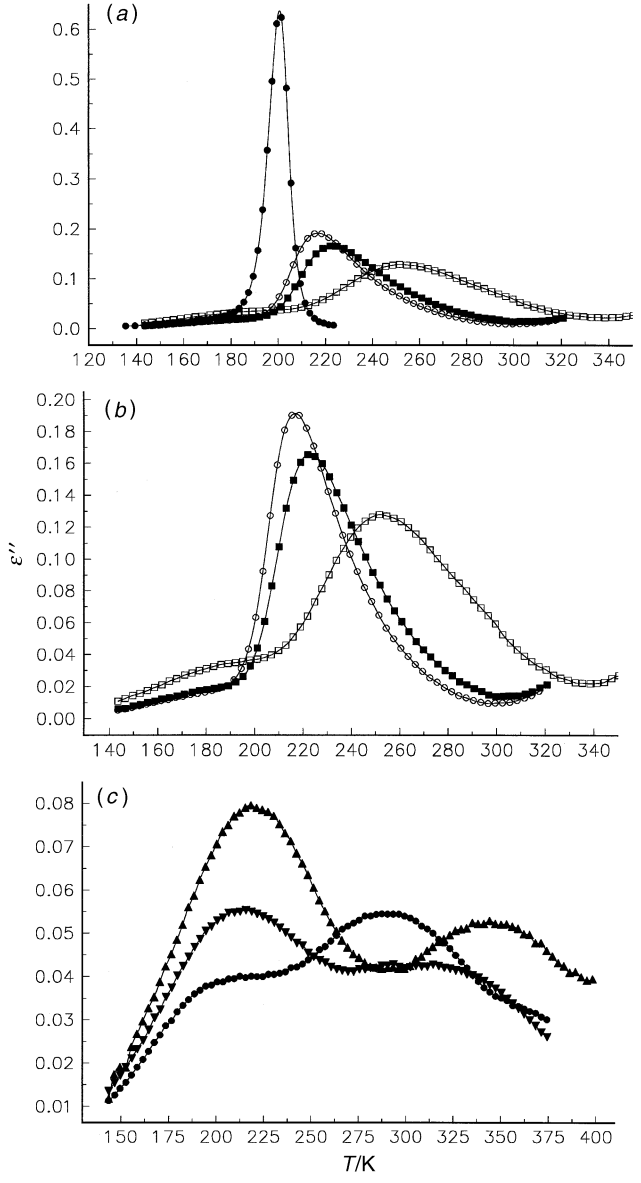

Fig. 6 Comparison of the loss factor temperature profiles: (*a*) for the monomer (●) and P1 (○), P2 (■) and P3 (□); (*b*) for P1 (○), P2 (■) and P3 (□); and (*c*) for P4 (●), P5 (▼) and P6 (▲), all measured at a frequency of 1 kHz

centred at *ca.* 180 K. Fig. 6(*c*) shows the loss plots for P4, P5 and P6; the β-process continues to grow and moves slightly to higher temperatures while the α-process is now of small magnitude and its peak position moves markedly to higher temperatures, being centred at 350 K for the most cured sample P6. The α-process moves from 195 to 350 K on going from the monomer to the fully cured glassy product P6. Its appearance for the uncured monomer is consistent with the normal α-relaxation observed in glass-forming liquids, which is characterised by the Vogel–Fulcher law for the dependence of the average relaxation frequency with temperature[8] and the Kohlrausch–Williams–Watt (KWW) relaxation function[17–19] with spread parameter $\bar{\beta}=0.55$. However, as we cure the samples to greater extents the loss curves for the α-process broaden remarkably and shift by 150 K to higher temperatures (Fig. 6). This clearly implies a change in mechanism on curing through the series of samples. At the same time the β-process, which is absent for the monomer, appears on curing and is a larger feature than that for the α-process in the highly cured samples [Fig. 6(c)].

It is well known that permittivity and loss data are frequency- and temperature-dependent for amorphous polymers.[13] In the present case, the plots of ε'' *vs.* T for fixed frequencies act as a fingerprint for the condition of a particular sample and may act as a guide for processing of the material from monomer to cross-linked polymer product. Fig. 7 shows the fingerprint loss spectra of two samples cured under identical conditions. P5 was made according to Table 1 using a fresh monomer–initiator mixture, while the 'aged' product was made using a monomer–initiator mixture that had been stored for six months at −10 °C in a refrigerator prior to curing. The differences are evident. First, the β-peak is smaller than the α-peak for the aged specimen while the reverse is true for P5. Secondly, the β-peak for the aged sample is smaller than that for P5, while the reverse is true for the α-process. Furthermore, the α- and β-processes for the aged sample peak at lower temperatures than those for P5. These results all show that the aged sample is not cured to the same extent as P5. The storage of the reaction mixture for this length of time clearly has reduced the effectiveness of the free-radical initiator and led to this result. Thus an important conclusion of this work is that the physical condition of cured samples may be compared with those of fully cured samples *via* plots of ε'' *vs.* T, as shown in Fig. 7.

Thus far we have described plots of ε'' *vs.* T for constant frequencies. As indicated above, we have reported previously[8] plots of ε' and ε'' *vs.* log(f/Hz) for the CR39 monomer that show KWW behaviour with $\bar{\beta}=0.55$. Fig. 8(*a*) and (*b*) shows plots of ε' and ε'' *vs.* log(f/Hz) respectively for P1. The loss curves are broad and become broader as the temperature is

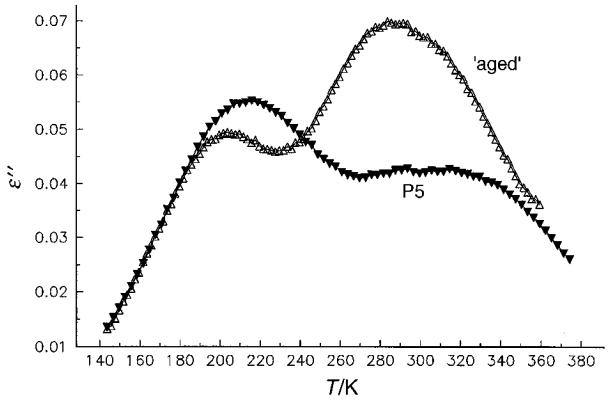

Fig. 7 Comparison of the loss factor temperature profiles (measured at a frequency of 1 kHz) for two products obtained at the same time in the cure cycle. The 'aged' product was obtained using a stock solution of reaction mixture that had been stored for six months prior to curing.

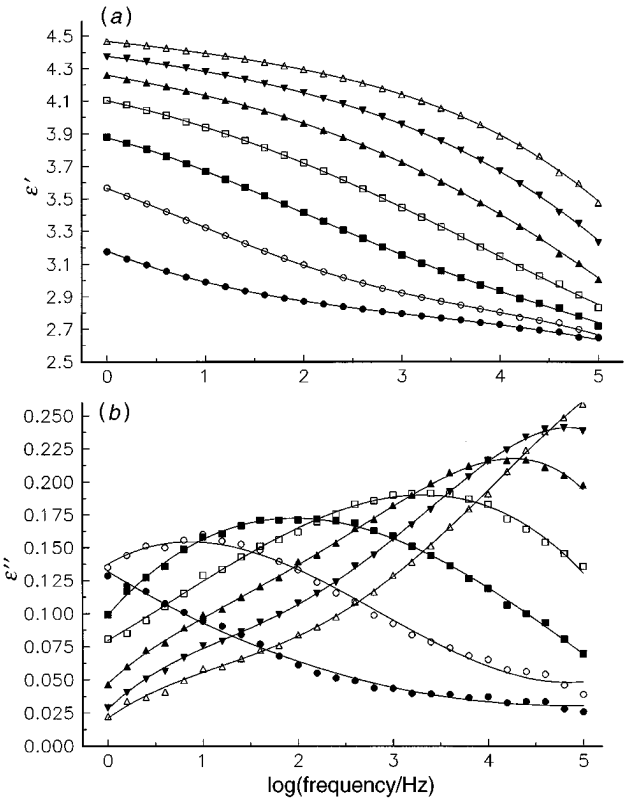

Fig. 8 (*a*) Permittivity (△, −40; ▼, −46; ▲, −52; □, −58; ■, −64; ○, −70; ●, −76 °C) and (*b*) loss factor (●, −40; ○, −46; ■, −52; □, −58; ▲, −64; ▼, −70; △, −76 °C) measured as a function of frequency for the least cured product, P1

decreased. The half-widths of the loss curves shown in Fig. 8(*b*) are in excess of four decades of frequency, which compares with two decades of frequency for the CR39 monomer,[8] and would correspond to KWW $\bar{\beta}$ values less than 0.25. These data [and those of Fig. 6(*a*) for P1] confirm that the α-relaxation mechanism is changed markedly when the cross-linked material is formed initially. Clearly, the cooperative motions of the ester and ether dipoles occur in a range of environments; hence the broadening seen in Fig. 8(*b*). The increased broadening of the loss curves with decreasing temperature is consistent with a spectrum of relaxation processes, each having their own apparent activation energy. The consequence is that the plots of log(f_m) *vs.* T^{-1} and log(f) *vs.* ${T_m}^{-1}$, where f_m is the frequency of maximum loss at a fixed temperature and T_{max} is the temperature of maximum loss at a fixed frequency, do not lie on a common curve. In practice, this means that for samples cured beyond P3 we cannot obtain reliable plots of log(f_m) *vs.* T^{-1} but are able to do so for plots of log(f) *vs.* ${T_{max}}^{-1}$ for all samples. Fig. 9 shows such plots for the α-process. The plots for P1–P3 are seen to be curved in the Vogel–Fulcher (VF) sense and all are shown to move strongly to higher temperatures, reflecting the increase in the T_g of the system that occurs as we proceed from uncured monomer through P1 to fully cured polymer P6. The VF equation [eqn. (1)] was fitted, using a computational reiterative procedure to produce a line of best fit, to the plots for P1, P2 and P3. The results are shown as the solid lines in the plots in Fig. 9 for these materials and the derived VF parameters from these plots are shown in Table 2. The quality of the fits shown is excellent for each data set, which is remarkable when it is remembered that the broadening of the curves is considerable on going from P1 to P3 [see Fig. 6(*b*)]. Using the parameters of eqn. (3) we calculated the apparent activation energies, Q_{app}, for different measuring frequencies for P1–P3

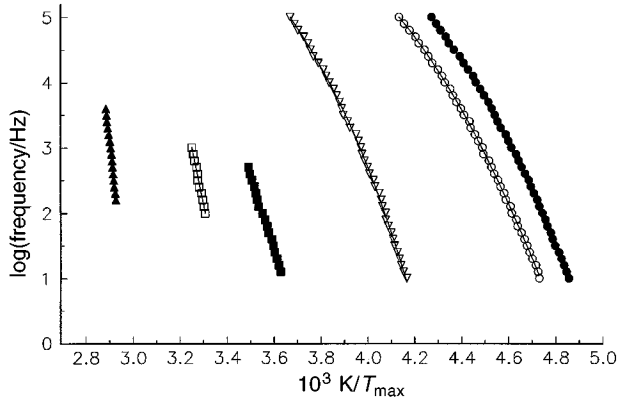

Fig. 9 Activation energy plots of log (frequency/Hz) *vs.* T_{max}^{-1} for the α-process for P1 (●), P2 (○), P3 (▽), P4 (■), P5 (□) and P6 (▲). The VF fits for P1–P3 and the Arrhenius fits for P4–P6 are shown as solid lines.

Table 2 Parameters of the Vogel–Fulcher relation fitted to the loss data in the temperature domain for the α-relaxation process of products P1–P3

product	B/K	T_o/K
P1	1077±1	161.0±0.1
P2	1164±4	162.7±0.1
P3	975±3	195.9±0.1

through the relation

$$Q_{app} = \frac{RB}{\left(1 - \frac{T_0}{T_{max}}\right)^2}; \qquad T \geqslant T_0 \tag{4}$$

and the results are given in Table 3. For each product it can be seen that as the frequency of measurement is decreased, the peak position of the loss curves decreases and the activation energy increases. Such an increase in Q_{app} is typical of that for α-relaxations in glass-forming liquids and amorphous polymers. Table 3 also shows that the apparent activation energies for the α-process of P1 and P2 at all frequencies of measurement are essentially the same. In comparison, those for P3 are increased appreciably.

We now consider the plots for products P4–P6 in Fig. 9. At low frequencies the α-process becomes overlapped by the ionic conductivity process for these materials which masks the α-loss peak position. At higher frequencies the α-process becomes overlapped by the lower temperature β-process, making definition of the loss peak positions for both processes difficult. The plots for P4–P6, therefore, appear as limited data lying about a straight line. In order to gain an indication of the effect of cure on the apparent activation energies for the α-process of these systems, the plots for P4–P6 shown in Fig. 9 were fitted to the Arrhenius relation given by eqn. (5),

$$\log(f) = f_0' - \frac{Q_{app}'}{RT_{max}} \tag{5}$$

where f_0' is an empirically determined constant and Q_{app}' is the apparent activation energy. The resulting fits for P4–P6 are shown as the solid lines in Fig. 9. Table 4 lists the Q_{app}' values calculated from the gradient of each of the lines. These values should be compared to the Q_{app} values shown in Table 3 for P1–P3 at a frequency of 10^3 Hz. During the later stages of reaction Table 4 shows that the activation energy of the α-relaxation process undergoes a further increase as we progress from the partially cured material P4 to the fully cured, highly cross-linked material P6. It should be remembered that all plots in Fig. 9 should show VF behaviour and converge to a common line at high temperatures when the bulk relaxation process is at frequencies in excess of *ca.* 10^{10} Hz. At such high temperatures, however, the materials will be chemically unstable.

Fig. 10 shows the corresponding plots of $\log(f)$ *vs.* T_{max}^{-1} for the β-process observed in each material. The linearity of each plot is excellent showing that the β-process obeys an Arrhenius equation and suggesting that the distribution of relaxation times is equivalent to a distribution of pre-exponential terms in the Arrhenius equation. As such, eqn. (5) was fitted to the plots in Fig. 10 and the results are shown as the solid lines in each case. The values of the apparent activation energies calculated from the slopes of the fits are given in Table 5. As the β-process moves to higher temperatures on increased curing so Q_{app}' increases. Note that a similar trend has been observed for the mechanical β-relaxation process observed in the dynamic mechanical studies on the effect

Table 4 Activation energies for the α-process for products P4–P6, calculated using the Arrhenius relation fitted to the plots shown in Fig. 9

product	Q'_{app}/kJ mol^{-1}
P4	213.8
P5	344.1
P6	614.0

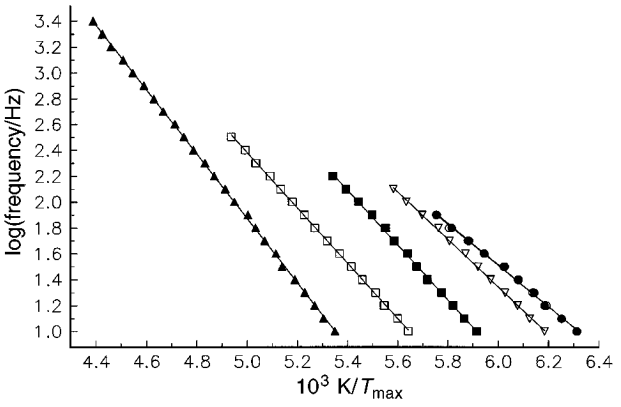

Fig. 10 Activation energy plots of log (frequency/Hz) *vs.* T_{max}^{-1} for the β-process for P1 (●), P2 (○), P3 (▽), P4 (■), P5 (□) and P6 (▲). The Arrhenius fits are shown as solid lines.

Table 3 Apparent activation energies (calculated using the VF parameters in Table 2) at each decade of frequency for the α-process of products P1–P3, together with the loss peak maxima

	P1		P2		P3	
log (f/Hz)	T_{max}/K	Q_{app}/kJ mol^{-1}	T_{max}/K	Q_{app}/kJ mol^{-1}	T_{max}/K	Q_{app}/kJ mol^{-1}
1	205.9	188.0	211.4	180.3	240.0	239.7
2	210.8	160.5	216.8	155.0	245.4	199.2
3	216.9	134.9	222.8	133.4	251.9	164.1
4	224.2	122.7	231.0	111.7	260.8	130.9
5	234.1	91.8	241.9	91.7	272.6	102.3

Table 5 Activation energies for the β-process for products P1–P6, calculated using the Arrhenius relation fitted to the plots shown in Fig. 10

product	Q'_{app}/kJ mol^{-1}
P1	30.9
P2	30.5
P3	35.2
P4	40.7
P5	41.1
P6	47.7

of increased cross-linking on molecular relaxations in di-epoxide–diamine systems studied by Charlesworth.[23,24] For amorphous polymers, local reorientational processes partially relax the auto- and cross-dipole moment correlation functions. The extent to which this occurs increases with increasing temperature.[13,16] This is also the case for the samples studied here. The remarkable feature of the present work is the increase in relaxation strength of the β-process as the extent of cure is increased. De Meuse[5] observed a strong β-process for two cured CR39 monomer samples made using benzyl peroxide as initiator. Note also that Mangion and Johari[20–22] studied the changes in dielectric behaviour of a diepoxide–diamine system. In addition to the changes in the frequency–temperature location of the α-process, they observed a β-process which for their DGEBA–DDM system increased in height and shifted to higher temperatures, while for their DGEBA–DDS system it increased in height but shifted to lower temperatures on curing. They interpreted their data for the β-process in terms of changes in the local environment of the regions surrounding the dipole segments. The difference in behaviour of the DDS and DDM systems is difficult to ascertain in terms of molecular structure.

Conclusions

By studying a series of samples ranging from the uncured monomer to the cured polymer over wide ranges of frequency and temperature, a complex pattern of behaviour has been revealed which may be summarised as follows.

(i) The simple α-process observed for this monomer transforms on curing to a broad feature that moves to higher temperatures and broadens considerably, to the extent that the α-process of monomer and polymer should be regarded as having very different mechanisms. That for the cured polymer corresponds to micro-Brownian motions of units in a range of environments and suggests that the cured network is heterogeneous at the mesoscopic level with local heterogeneities smaller that the wavelength of light. While the α-process is extremely broad in plots of ε'' *vs.* log(f/Hz) for partially cured materials, the corresponding plots of ε'' *vs.* T clearly show the location of the α-process and hence allow Fig. 9 to be constructed, which shows the shift of the α-process to higher temperatures and its sustained large apparent activation energy in cured samples.

(ii) The β-process that emerges in the range 180–230 K (see Fig. 6) is a surprising observation. As the network is formed the localised motions of the dipolar groups at these low temperatures increase in activity. The origin of this behaviour is unclear. One may speculate that at long cure times, the continual reaction, leading to new polymer chains and increased cross-linking, is accompanied by physical annealing of the material which changes the environment of the ether and ester groups to give them additional freedom compared with the situation at earlier times. Certainly one result of this work is that the dielectric absorption spectra act as a clear diagnostic fingerprint of the extent to which cure has been achieved and is of practical use to compare different cured products (see Fig. 6 and 7).

The authors gratefully acknowledge the provision of a grant from the EPSRC for the purchase of the dielectric spectrometer and for the award of a PDRA to S.A. and a case studentship to I.K.S.

References

1 W. R. Dial, W. E. Bissinger, B. J. DeWitt and F. Strain., *Ind. Eng. Chem.*, 1955, **47**, 2447.
2 E. Schnarr and K. Russell, *J. Polym. Sci.*, 1980, **18**, 913.
3 H. W. Starkweather and F. R. Eirich, *Ind. Eng. Chem.*, 1955, **47**, 2452.
4 D. J. T. Hill, D. I. Londero, J. H. O'Donnell and P. J. Pomery, *Eur. Polym. J.*, 1990, **26**, 1157.
5 M. De Meuse, *Polym. Eng. Sci.*, 1993, **33**, 1049.
6 M. De Meuse, *J. Polym. Sci., B Polym. Phys.*, 1994, **32**, 1749.
7 M. Frounchi, R. P. Chaplin and R. P. Burford, *Polymer*, 1994, **35**, 752.
8 I. K. Smith, S. R. Andrews, G. Williams and P. A. Holmes, *J. Mater. Chem.*, 1996, **6**, 539.
9 T. Holt and W. Simpson, *Proc. R. Soc. London A*, 1956, **238**, 156.
10 A. Matsuoto and M. Iowa, *J. Polym. Sci., Part A-1*, 1970, **8**, 751.
11 A. Matsuoto and M. Iowa, *J. Polym. Sci., Polym. Chem.*, 1976, **14**, 2383.
12 L. K. Kostanski and W. Krolinkowski, *J. Polym. Sci., Polym. Chem.*, 1985, **23**, 605.
13 N. G. McCrum, B. E. Read and G. Williams, *Anelastic and Dielectric Effects in Polymeric Solids*, Dover Publications, New York, 1991.
14 G. Williams, *Chem. Rev.*, 1972, **72**, 55.
15 G. Williams, *Chem. Soc. Rev.*, 1978, **7**, 89.
16 G. Williams, *Adv. Polym. Sci.*, 1979, **33**, 59.
17 R. Kohlrausch, *Pogg. Ann. Phys.*, 1854, **4**, 77.
18 G. Williams and D. C. Watts, *Trans. Faraday. Soc.*, 1970, **66**, 80.
19 G. Williams, D. C. Watts, S. B. Dev and A. M. North, *Trans. Faraday. Soc.*, 1971, **67**, 1323.
20 M. B. M. Mangion and G. P. Johari, *J. Polym. Sci., Part B, Polym. Phys.*, 1990, **28**, 71.
21 M. B. M. Mangion and G. P. Johari, *J. Polym. Sci., Part B, Polym. Phys.*, 1991, **29**, 437.
22 M. B. M. Mangion and G. P. Johari, *Macromolecules*, 1990, **23**, 3687.
23 J. M. Charlesworth, *Polym. Eng. Sci.*, 1988, **28**, 221.
24 J. M. Charlesworth, *Polym. Eng. Sci.*, 1988, **28**, 230.

Paper 6/06296B; *Received* 12*th September*, 1996